DOI:10.3969/j.issn.1001-5485.2013.08.021 2013,30(08):97-101

一种 Godunov 算法及其在非平底流污染物传输中的应用

杨金波[1],段文刚[1],黄国兵[1],李订芳[2]
(1. 长江科学院 水力学研究所,武汉 430010;2. 武汉大学 数学与统计学院,武汉 430072)

摘要:采用和谐的加权平均通量(Weighted Average Flux,简称 WAF)算法,研究了浅水波方程的间断解及污染物传输问题。该算法采用 WAF 格式和 HLLC Riemann 求解器近似单元边界数值通量,中心差分格式离散地形源项,然后理论上证明了该算法是和谐的。最后利用 WAF 算法对非平底地形上浅水波间断解及污染物传输问题进行数值计算,精确地捕捉到了间断解和污染物运动过程,结果表明该算法满足守恒性,具有高分辨率、无振荡及捕捉污染物运动边界的能力。

关 键 词:浅水波方程;WAF 格式;溃坝;污染物传输
中图分类号:X52 **文献标志码**:A **文章编号**:1001-5485(2013)08-0097-05

1 研究背景

河流、湖泊和近海岸的污染问题越来越严重,一方面破坏了生态环境;另一方面对人类生命安全和经济发展带来致命性的危害,因此有必要研究污染物传输方式的数学模型。

污染物传输的数值算法包括浅水波和污染物传输扩散的计算。在浅水波方程计算方面,近年来空气动力学中的 Godunov[1] 型有限体积算法越来越普遍地应用到浅水波方程中,WAF 方法[2] 是 Toro 基于 Godunov 思想提出的显示、二次精度的守恒有限体积格式。非平底河床是浅水方程计算的一个关键问题,为了构造和谐的数值格式,Roe[3] 提出迎风离散双曲型方程中源项的思想;Bermudez 和 Vazquez-Cendon[4] 用迎风离散源项的方法计算了浅水波方程;Hubbard 和 Garcia-Navarro[5] 用迎风离散源项的方法构造了平衡源项和通量梯度的二阶格式;Zhou[6] 等人对二维浅水波方程提出了水位梯度法。对于污染物传输部分,考虑对流占优的问题,文章采用垂直方向平均的传输方程,忽略了扩散项。数值求解时,污染物传输方程作为整个系统的一个波系,同浅水方程耦合求解。

本文首先构造了浅水波方程和污染物扩散方程的二阶精度和谐 WAF 格式,然后用该算法研究了非平底河床上浅水流的间断解及污染物传输问题,将计算结果同精确解或其他文献比对,证明该方法的计算结果精度高、分辨率高,能计算真实的溃坝和污染物传输问题。

2 数值格式

2.1 浅水波及污染物传输方程

控制方程由浅水波方程和污染物运输方程组成,其中,污染物部分主要研究污染物传输过程,忽略污染物扩散项,如

$$\frac{\partial \boldsymbol{U}}{\partial t}+\frac{\partial \boldsymbol{F}}{\partial x}=S \quad 。 \tag{1}$$

其中:

$$\boldsymbol{U}=\begin{pmatrix} H \\ q \\ r \end{pmatrix} \quad ; \quad \boldsymbol{F}=\begin{pmatrix} q \\ q^2/h+gH/2-gHb \\ qr/h \end{pmatrix} \quad ;$$

$$\boldsymbol{S}=\begin{pmatrix} 0 \\ -gh\dfrac{\partial b}{\partial x} \\ 0 \end{pmatrix} \quad 。$$

式中:$H=h+b(x)$ 为水位高程;h 为水深,$b(x)$ 为河床高程;$q=hu$ 为单宽流量;u 为流速,传输标量 $r=hc$;c 为污染物浓度;g 为重力加速度。

2.2 WAF 有限体积格式

对式(1)关于区间 $[x_{i-1/2},\ x_{i+1/2}]\times[\ t^n,\ t^{n+1}]$

收稿日期:2013-04-16;修回日期:2013-06-19
基金项目:国家自然科学基金资助项目(11102027);中央级基本科研业务费项目(CKSF2011014/SL,CKSF2013025/SL,CKSF2012010/SL)
作者简介:杨金波(1982-),男,山东德州人,工程师,博士,主要从事计算流体力学,(电话)027-82823698(电子信箱)yangjb1225@163.com。

积分,并应用格林(Green)公式,则得有限体

$$U_i^{n+1} = U_i^n - \frac{\Delta t}{\Delta x}(F_{i+1/2}^n - F_{i-1/2}^n) + \frac{\Delta t}{\Delta x}S_i^n \quad 。(2)$$

式中:U_i^n 为解 $U(x,t^n)$ 在单元 I_i 内的空间平均,$F_{i+1/2}^n$ 为单元边界 $x_{i+1/2}$ 处的数值通量;S_i^n 为数值源项,这里采用 TVD-WAF 格式给出数值通量,中心差分格式离散源项。如图 1 所示,假设局部 Riemann 问题自相似解仅有激波结构,TVD-WAF 格式[7]的数值通量为

$$F_{i+1/2}^{\mathrm{WAF}} = \frac{1}{2}(F_i + F_{i+1}) - \frac{1}{2}\sum_{k=1}^{N}\mathrm{sign}(c_k)\phi_{i+1/2}^{(k)}\Delta F_{i+1/2}^{(k)} 。 \quad (3)$$

式中:$\Delta F_{i+1/2}^{(k)} = F_{i+1/2}^{(k)} - F_{i+1/2}^{(k-1)}$ 为第 k 个波处通量的跳量;$F_i = F(U_i^n)$ 和 $F_{i+1} = F(U_{i+1}^n)$;$N=3$ 为波数;$c_k = S_k\Delta t/\Delta x$ 为波速 S_k 的 courant 数;sign(c)为符号函数;$\phi(c)$为通量限制函数[8]。

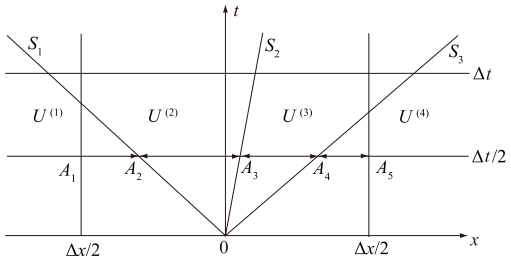


图 1 局部 Riemann 问题自相似解的波结构
Fig. 1 Wave structure of self-similar solution for local Riemann problem

$$\phi(r^{(k)},c_k) = \begin{cases} 1, & r^{(k)} \leqslant 0; \\ 1 - \dfrac{(1 - |c_k|)r^{(k)}(1 + r^{(k)})}{1 + r^{(k)2}}, & r^{(k)} > 0。 \end{cases}$$

其中:

$$r^{(k)} = \begin{cases} \dfrac{p_i^{(k)} - p_{i-1}^{(k)}}{p_{i+1}^{(k)} - p_i^{(k)}}, & S_k \geqslant 0; \\ \dfrac{p_{i+2}^{(k)} - p_{i+1}^{(k)}}{p_{i+1}^{(k)} - p_i^{(k)}}, & S_k < 0 。 \end{cases} \quad (4)$$

式(4)中变量 p 可以为任意一个在波 k 处变化的物理量,这里取 $p^{(k)} = H, k = 1,3\cdots; p^{(2)} = r, k = 2$。

为了计算 $F_{i+1/2}^{\mathrm{WAF}}$,采用 HLLC 解法器[6]来近似 Riemann 问题自相似解的中间状态,

$$[F^{\mathrm{HLLC}}]_{(k)} = [F^{\mathrm{HLL}}]_{(k)}, \quad k = 1,2;$$

$$[F^{\mathrm{HLLC}}]_{(3)} = \begin{cases} [F^{\mathrm{HLLC}}]_{(1)}v_l, & S_2 > 0; \\ [F^{\mathrm{HLLC}}]_{(1)}v_R, & S_2 < 0 。 \end{cases} \quad (5)$$

下标(k)表示通量向量的第 k 项,其中 HLL 求解器定义为

$$F^{\mathrm{HLL}} = \begin{cases} F_i, & S_1 \geqslant 0; \\ \dfrac{S_3F_i - S_1F_{i+1} + S_1S_3(U_{i+1} - U_i)}{S_3 - S_1}, & S_1 < 0 \leqslant S_3; \\ F_{i+1}, & S_3 \leqslant 0 。 \end{cases} \quad (6)$$

左右波速度 S_1 和 S_3 通过文献[7]给出,即

$$\begin{cases} S_1 = \min(u_i - \sqrt{gh_i}, u_s - \sqrt{gh_s}), \\ S_3 = \max(u_{i+1} + \sqrt{gh_{i+1}}, u_s + \sqrt{gh_s}) 。 \end{cases} \quad (7)$$

式中

$$u_s = (u_i + u_{i+1})/2 + \sqrt{gh_i} - \sqrt{gh_{i+1}};$$

$$\sqrt{gh_s} = (\sqrt{gh_i} + \sqrt{gh_{i+1}})/2 + (u_i - u_{i+1})/4 。$$

对于接触间断波的波速 S_2[7]的估计为

$$S_2 = \frac{S_1h_1(u_{i+1} - S_3) - S_3h_{i+1}(u_i - S_1)}{h_i(u_{i+1} - S_3) - h_{i+1}(u_i - S_1)} 。 \quad (8)$$

当出现干湿边界时 S_1, S_3 分别调整:

左干河床

$$S_1 = u_{i+1} - 2\sqrt{gh_{i+1}}, \quad S_2 = u_{i+1} + \sqrt{gh_{i+1}} 。 \quad (9)$$

右干河床

$$S_1 = u_i - \sqrt{gh_i}, \quad S_2 = u_i + 2\sqrt{gh_i} 。 \quad (10)$$

此时,式(8)中的 S_3 会自动和估计的干河床式(9)或式(10)重合。

为保证数值格式的稳定性,时间步长

$$\Delta t = \mathrm{CFL}\frac{\Delta x}{\max\limits_{1\leqslant i\leqslant M}\max(|u_i - \sqrt{gh_i}|, |u_{i+1} + \sqrt{gh_{i+1}}|)} 。 \quad (11)$$

其中 CFL($0 < \mathrm{CFL} \leqslant 1$)是 Courant 数。

地形源项采用中心差分格式进行离散

$$-\int_{x_{i-1/2}}^{x_{i+1/2}} gH\frac{\partial b}{\partial x}\mathrm{d}x = -gH_i(b|_{x_{i+1/2}} - b|_{x_{i-1/2}}) 。 \quad (12)$$

2.3 和谐性质证明

为了证明 WAF 格式的和谐性,只需证明静态条件 $q = 0$ m,H = 常数及 r = 常数时,下式成立

$$F_{i+1/2} - F_{i-1/2} = S_i^n 。 \quad (13)$$

由 TVD-WAF 格式的数值通量定义式(3)和静水条件,单元 I_i 右边界 $x_{i+1/2}$ 处的数值通量为

$$F_{i+1/2}^{\mathrm{WAF}} = \{\frac{1}{2}(F_i + F_{i+1}) - \frac{1}{2}[\mathrm{sign}(c_1)\phi_{i+1/2}^{(1)}(F_L^{\mathrm{HLLC}} - F_i) + \mathrm{sign}(c_2)\phi_{i+1/2}^{(2)}(F_R^{\mathrm{HLLC}} - F_L^{\mathrm{HLLC}}) +$$

$$\mathrm{sign}(c_3)\phi^{(3)}_{i+1/2}(F_{i+1}-F^{\mathrm{HLLC}}_R)]\}_{i+1/2}=\begin{pmatrix}0\\ \frac{1}{2}\left[\frac{1}{2}(gH^2-gHb_{i+1/2})+(\frac{1}{2}gH^2-gHb_{i+1/2})\right]\\ 0\end{pmatrix}=\begin{pmatrix}0\\ \frac{1}{2}gH^2-gHb_{i+1/2}\\ 0\end{pmatrix}。\tag{14}$$

同理在 $x_{i-1/2}$ 处的数值通量为

$$F^{\mathrm{WAF}}_{i-1/2}=\left\{\frac{1}{2}(F_{i-1}+F_i)-\frac{1}{2}[\mathrm{sign}(c_1)\phi^{(1)}_{i-1/2}(F^{\mathrm{HLLC}}_L-F_{i-1})+\mathrm{sign}(c_2)\phi^{(2)}_{i-1/2}(F^{\mathrm{HLLC}}_R-F^{\mathrm{HLLC}}_L)+\mathrm{sign}(c_3)\phi^{(3)}_{i-1/2}(F_i-F^{\mathrm{HLLC}}_R)]\right\}_{i-1/2}=\begin{pmatrix}0\\ \frac{1}{2}\left[\frac{1}{2}(gH^2-gHb_{i-1/2})+(\frac{1}{2}gH^2-gHb_{i-1/2})\right]\\ 0\end{pmatrix}=\begin{pmatrix}0\\ \frac{1}{2}gH^2-gHb_{i-1/2}\\ 0\end{pmatrix}。\tag{15}$$

同时由数值源项的定义式(12)

$$-\int_{x_{i-1/2}}^{x_{i+1/2}}gH\frac{\partial b}{\partial x}\mathrm{d}x=-gH(bx_{i+1/2}-b_{x_{i-1/2}})。\tag{16}$$

将式(14),式(15)和式(16)分别代入式(13)很清楚地证明格式满足和谐性。

3　算　例

这里利用 WAF 格式对非平底间断浅水波方程中污染物传输问题进行了数值计算,研究了溃坝波传播过程中污染物的传输过程和机理,试验结果表明该算法可以精确地捕捉激波和污染物传输边界,无振荡。

3.1　梯形河床上的污染物传输问题

本算例[8]梯形河床定义为

$$b(x)=\begin{cases}4.5\ \mathrm{m}, & x>2\ \mathrm{m};\\ 0, & x<2\ \mathrm{m}。\end{cases}$$

初始条件为

$$H_0=18\ \mathrm{m},\ q_0=18-b(x);\quad r_0=\begin{cases}18-b(x), & x>2\ \mathrm{m},\\ 0, & x<2\ \mathrm{m}。\end{cases}\tag{17}$$

计算步长 $\Delta x=0.08$ m,CFL = 0.9。$T=1$ s 时计算结果如图 2 所示。WAF 算法计算的水位和 HLLC 格式计算的水位吻合较好,同时由图 3 可知,WAF 格式对污染物运动的计算比一阶精度的 HLLC 格式分辨率要高,WAF 算法的计算数值耗散低。

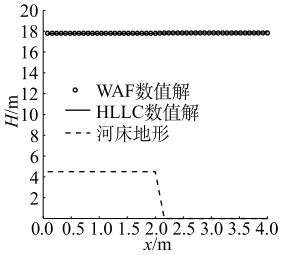


图 2　水面线

Fig. 2　Water surface profile

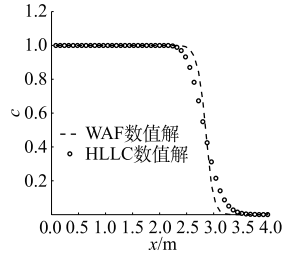


图 3 污染物分布

Fig. 3　Pollutant distribution

3.2　溃坝波中的污染物传输问题

本算例研究了溃坝过程中污染物传输规律,计算区域为 2 000 m 长的平底无摩擦河道,溃坝初始条件如下:

$$H_0=\begin{cases}1\ \mathrm{m}, & x<1\ 000\ \mathrm{m},\\ 0.5\ \mathrm{m}, & x>1\ 000\ \mathrm{m},\end{cases}\quad q=0;\qquad r_0=\begin{cases}0.7, & x<900\ \mathrm{m},\\ 0.9, & 900\ \mathrm{m}<x<1\ 000\ \mathrm{m},\\ 0.25, & x>1\ 000\ \mathrm{m}。\end{cases}\tag{18}$$

采用 100 个计算单元,CFL = 0.9。$T=250$ s 时计算水位和单宽流量如图 4 所示,可以看出 WAF 格式比 HLLC 格式计算的更逼近解析解。在污染物计算方面,如图 5,WAF 计算的污染物区域比 HLLC 格式窄,浓度更高,说明 WAF 比 HLLC 在数值计算方面的耗散低,精度高。

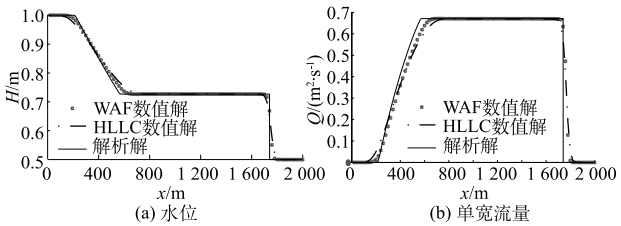


图 4　水位和单宽流量

Fig. 4　Water level and discharge per unit width

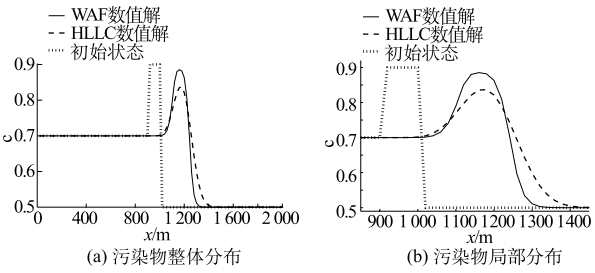


图 5　污染物中心分布

Fig. 5　Distribution of pollutant center

3.3　带干湿河床的污染物传输问题

该算例利用 WAF 算法研究干湿河床上的污染

物传输问题[9],初始条件为:

$$H_0 = 10\ \text{m},\quad q_0 = \begin{cases} 350\ \text{m}^3/\text{s}, & x < 50/3, \\ -350\ \text{m}^3/\text{s}, & \text{其它}。 \end{cases}$$

$$r_0 = \begin{cases} H_0 - b(x), & 25/3\ \text{m} < x < 12.5\ \text{m}, \\ 0, & \text{其它}。 \end{cases} \tag{19}$$

其中地形定义为

$$b(x) = \begin{cases} 1\ \text{m}, & 25/3\ \text{m} < x < 12.5\ \text{m}, \\ 0, & \text{其它}。 \end{cases}$$

空间步长 $\Delta x = 0.1$ m, CFL = 0.8。$t = 0.25$ s 时,计算结果如图 6 所示。WAF 格式计算的水位能很好的和参考值吻合(该算例没有解析解,可采用 HLLC 格式在 2 000 个网格下的计算结果作为参考值)。并且精确地捕捉到阻碍物左边 $x = 25/3$ m 处的激波和 $x = 6.5$ m处的水面涌起。同时,分析 $t = 0.18$ s时污染物运动状态,如图 7。可以看出 WAF 比 HLLC 格式精度高。进一步,由初始条件产生的向左和向右运动的 2 个稀疏波中间形成干河床,改进后的 WAF 算法可以很好处理干湿边界问题。该算例说明 WAF 算法具有高精度、高分辨率,及能处理复杂干河床问题,具有真实问题的处理能力。

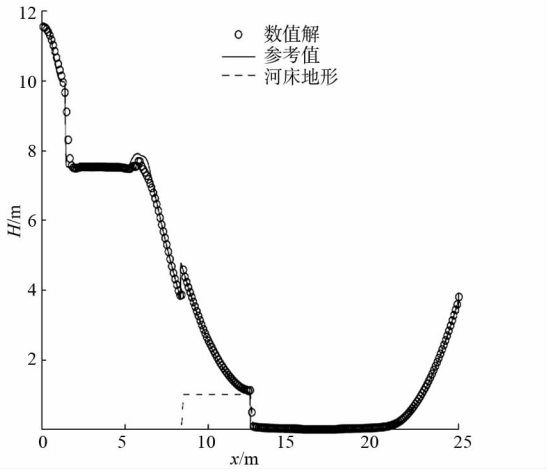


图 6 $T = 0.25$ s 时刻水面线

Fig. 6 Water surface profile at $T = 0.25$ s

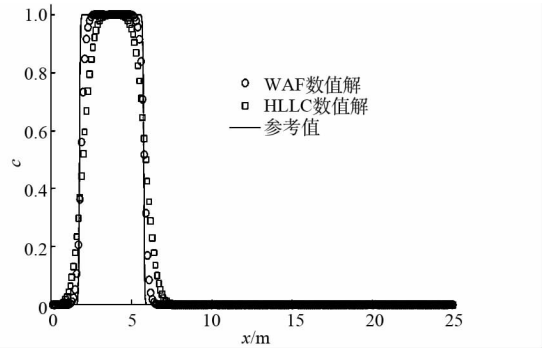


图 7 $T = 0.18$ s 时污染物分布

Fig. 7 Pollutant distribution at $T = 0.18$ s

4 结 语

本文利用二阶精度和谐 WAF 格式研究了浅水波方程和污染物扩散问题,研究了污染物在溃坝、非平底河床情况下的传播机理计算结果同精确解或其他文献比对,证明该方法是高精度、高分辨率,能计算真实的溃坝和污染物传输问题。

参考文献:

[1] GODUNOV S K. Finite Difference Methods for the Computation of Discontinuous Solutions of the Equations of Fluid Dynamics [J]. Matematicheskiĭ Sbornik, 1959, 47: 271 – 306.

[2] TORO E F. A Weighted Average Flux Method for Hyperbolic Conservation Laws [J]. Proceedings of the Royal Society A: Mathematical, Physical and Engineering Sciences, 1989, 423(1865): 401 – 418.

[3] ROE L P. Upwind Differencing Schemes for Hyperbolic Conservation Laws with Source Terms [C] // Springer-Verlag. Proceedings of an Advanced Research Workshop: Nonlinear Hyperbolic Problems: Lecture Notes in Mathematics, Volume 1270. St. Etienne, France January 13 – 17, 1986: 41 – 51.

[4] BERMUDEZ A, VAZQUEZ-CENDON E M. Upwind Methods for Hyperbolic Conservation Laws with Source Terms [J]. Computers and Fluids, 1994, 23(8): 1049 – 1071.

[5] HUBBARD E M, GARCIA-NAVARRO P. Flux Difference Splitting and the Balancing of Source Terms and Flux Gradients [J]. Journal of Computational Physics, 2001, 165(1): 89 – 125.

[6] ZHOU G J, CAUSON M D, MINGHAN G C, *et al*. The Surface Gradient Method for the Treatment of Source Terms in the Shallow-Water Equations [J]. Journal of Computational Physics, 2001, 168(1): 1 – 25.

[7] GALLOUËT T, HÉRARD J M, SEGUIN N. Some Approximate Godunov Schemes to Compute Shallow Water Equations with Topography [J]. Computers and Fluids, 2003, 32(4): 479 – 513.

[8] TORO E F. Shock-Capturing Methods for Free-Surface Shallow Flows [M]. Chichester: Wiley, 2001.

[9] FERNANDEZ-NIETO E D, NARBONA-REINA G. Extension of WAF Type Methods to Non-homogeneous Shallow Water Equations with Pollutant [J]. Journal of Scientific Computing, 2008, 36(2): 193 – 217.

(编辑:王 慰)

Application of a Godunov-Type Algorithm to the Pollutant Transport with Irregular Bedslope

YANG Jin-bo[1], DUAN Wen-gang[1], HUANG Guo-bing[1], LI Ding-fang[2]
(1. Hydraulics Department, Yangtze River Scientific Research Institute, Wuhan 430010, China;
2. School of Mathematics and Statistics, Wuhan University, Wuhan 430072, China)

Abstract: A well-balanced weighted average flux (WAF) scheme is proposed for the nonhomogeneous shallow water equations with pollutant transport. The water surface elevation and water discharge are used as the conserved variables in the shallow water equations, while the conserved variables and the bed elevation are set on the staggered mesh. Here, the WAF scheme combined with the HLLC Riemann solver is directly performed for the nonhomogeneous shallow water equations with pollutant transport, and the spatial second order central difference approximation is applied to source terms. Then, it's proved that the extended WAF scheme is harmonious in theory. Finally, several numerical tests about the steady and nonsteady flows over the irregular bottom or with the wet/dry front are simulated. The results obviously suggest that the WAF scheme is a well-balanced, robust, efficient, and practical scheme with high resolution.

Key words: shallow water equations; WAF scheme; dam-break; pollutant transport

(上接第 96 页)

Influencing Factors of Water Temperature Variation near Downstream Gezhouba Dam in the Yangtze River

XING Ling-hang, LIU Meng-kai, HUANG Guo-bing
(Hydraulics Department, Yangtze River Scientific Research Institute, Wuhan 430010, China)

Abstract: Researches on the influencing factors of water temperature variation near downstream Gezhouba dam would be conducive to understand the nature of water temperature variation, and is of great significance for the protection of Chinese sturgeon spawning grounds. In the present research, one-dimensional mathematical model of water flow and temperature together with the overall heat budget balance is adopted to preliminarily research this issue. Results reveal that the water temperature near downstream Gezhouba dam is mainly affected by the water temperature in the Three Gorges Reservoir; while other factors such as the inflow heat from Cuntan, the outflow heat from Three Gorges Dam and the operation mode of Gezhouba hydropower station have relatively less impacts. To be specific, net radiation heat and vaporization heat dominated the yearly variation of water temperature in the reservoir both before and after the operation of TGP, but the contribution of air-water heat conduction increased remarkably after the TGP operation. In November, particularly, heat conduction was the main influencing factor before and after TGP, but after the operation of TGP with the raising of impoundment level, the proportion of radiation heat and vaporization heat increased obviously, whereas heat conduction, inflow heat from Cuntan, and outflow heat from Three Gorges Dam gradually weakened. The operation of TGP have impacts on the contribution of each factor, hence affecting the water temperature in downstream Gezhouba dam.

Key words: Three Gorges Project; one-dimensional model of water flow and temperature; water temperature variation